LETTER

doi:10.1038/nature11472

Quantum teleportation over 143 kilometres using active feed-forward

Xiao-Song Ma[1,2]†, Thomas Herbst[1,2], Thomas Scheidl[1], Daqing Wang[1], Sebastian Kropatschek[1], William Naylor[1], Bernhard Wittmann[1,2], Alexandra Mech[1,2], Johannes Kofler[1,3], Elena Anisimova[4], Vadim Makarov[4], Thomas Jennewein[1,4], Rupert Ursin[1] & Anton Zeilinger[1,2]

The quantum internet[1] is predicted to be the next-generation information processing platform, promising secure communication[2,3] and an exponential speed-up in distributed computation[2,4]. The distribution of single qubits over large distances via quantum teleportation[5] is a key ingredient for realizing such a global platform. By using quantum teleportation, unknown quantum states can be transferred over arbitrary distances to a party whose location is unknown. Since the first experimental demonstrations of quantum teleportation of independent external qubits[6], an internal qubit[7] and squeezed states[8], researchers have progressively extended the communication distance. Usually this occurs without active feed-forward of the classical Bell-state measurement result, which is an essential ingredient in future applications such as communication between quantum computers. The benchmark for a global quantum internet is quantum teleportation of independent qubits over a free-space link whose attenuation corresponds to the path between a satellite and a ground station. Here we report such an experiment, using active feed-forward in real time. The experiment uses two free-space optical links, quantum and classical, over 143 kilometres between the two Canary Islands of La Palma and Tenerife. To achieve this, we combine advanced techniques involving a frequency-uncorrelated polarization-entangled photon pair source, ultra-low-noise single-photon detectors and entanglement-assisted clock synchronization. The average teleported state fidelity is well beyond the classical limit[9] of two-thirds. Furthermore, we confirm the quality of the quantum teleportation procedure without feed-forward by complete quantum process tomography. Our experiment verifies the maturity and applicability of such technologies in real-world scenarios, in particular for future satellite-based quantum teleportation.

Significant progress has been made recently in the field of quantum communication based on optical free-space links[10–19], which potentially allow much larger propagation distances compared to the existing fibre networks because of the lower photon loss per kilometre. To enable quantum communication on a global scale and among parties not having access to any fibre network, it is foreseeable that experiments will involve ground-to-satellite[10,11,15] and inter-satellite links.

Previous experiments focused on the distribution of quantum states of single photons or entangled photon pairs over optical free-space links. However, the realization of more sophisticated multiphoton quantum information protocols, such as quantum teleportation, remained an experimental challenge under real-world conditions. Quantum teleportation is based on the simultaneous creation of at least three photons, which for random photon pair sources reduces the count rate by several orders of magnitude compared to experiments using only two photons[16,19]. This decreases the signal-to-noise ratio and requires a long integration time, such that high system stability is necessary. Moreover, the complexity and environmental requirements of a quantum teleportation set-up are increased significantly compared to previous two-photon experiments, which provides significant experimental and technological challenges. The work presented in ref. 18 was a significant achievement in long-distance quantum communication, harnessing the entanglement between different degrees of freedom of a single photon. However, because the teleported qubit was not provided independently from the outside, the applicability of that scheme is limited. Most earlier experiments on teleportation of qubits and squeezed states[6–8] were in-laboratory demonstrations, and hence the communication distances were rather short. Although fibre-based teleportation has been demonstrated experimentally[20,21], the maximum transmission distance is limited by the intrinsic photon loss in optical fibre, unless quantum repeaters are involved[22]. In comparison to these previous studies, the experiment presented in this Letter achieves long-distance free-space teleportation of an independent quantum state, thus paving the way for satellite-based global quantum communication.

Quantum teleportation relies on using both a quantum channel and a classical channel between two parties, usually called Alice and Bob[5] (here located in La Palma and Tenerife respectively; Fig. 1a). The quantum channel is used by Alice and Bob to share the entangled auxiliary state[23]

$$|\Psi^-\rangle_{23} = \frac{1}{\sqrt{2}}\left(|H\rangle_2|V\rangle_3 - |V\rangle_2|H\rangle_3\right) \quad (1)$$

which is one of the four maximally entangled Bell states ($|\Psi^\pm\rangle = \frac{1}{\sqrt{2}}(|H\rangle|V\rangle \pm |V\rangle|H\rangle)$ and $|\Phi^\pm\rangle = \frac{1}{\sqrt{2}}(|H\rangle|H\rangle \pm |V\rangle|V\rangle)$). $|H\rangle$ and $|V\rangle$ denote the horizontal and vertical polarization states. Alice and Bob share this entangled state, where photon 2 is with Alice and photon 3 is with Bob. Charlie provides the input photon 1 to be teleported to Alice in a general polarization state

$$|\phi\rangle_1 = \alpha|H\rangle_1 + \beta|V\rangle_1 \quad (2)$$

where α and β are complex numbers ($|\alpha|^2 + |\beta|^2 = 1$), unknown to both Alice and Bob.

Alice then performs a Bell-state measurement (BSM), projecting photons 1 and 2 randomly onto one of the four Bell states each with the same probability of 25%. As a consequence, photon 3 is projected onto the input state $|\phi\rangle$, up to a unitary transformation (**U**), which depends on the outcome of the BSM. When Alice feeds the outcome of the BSM forward to Bob via the classical channel, he can implement the corresponding unitary operation in real time and thus obtain photon 3 in the initial state (equation (2)) of photon 1. If $|\Psi^-\rangle_{12}$ is detected, then **U** corresponds to the identity operation, which means that Bob needs to do nothing. If, on the other hand, $|\Psi^+\rangle_{12}$ is detected, Bob has to apply a π phase shift between the horizontal and the vertical component of his photon 3.

[1]Institute for Quantum Optics and Quantum Information (IQOQI), Austrian Academy of Sciences, Boltzmanngasse 3, A-1090 Vienna, Austria. [2]Vienna Center for Quantum Science and Technology, Faculty of Physics, University of Vienna, Boltzmanngasse 5, A-1090 Vienna, Austria. [3]Max Planck Institute of Quantum Optics, Hans-Kopfermann-Straße 1, 85748 Garching/Munich, Germany. [4]Institute for Quantum Computing and Department of Physics and Astronomy, University of Waterloo, 200 University Avenue West, Waterloo, Ontario N2L 3G1, Canada. †Present address: Department of Electrical Engineering, Yale University, New Haven, Connecticut 06520, USA.

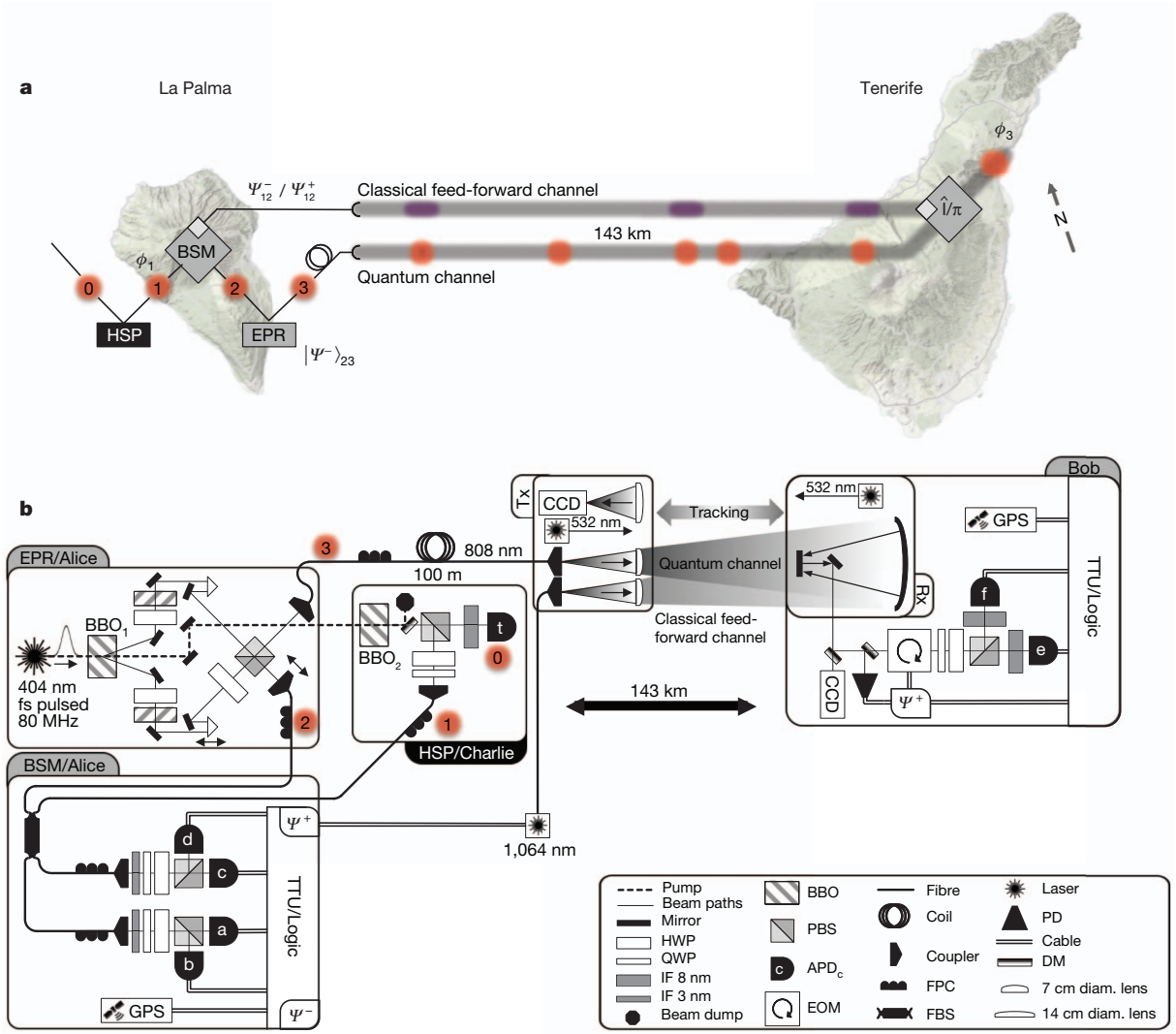

Figure 1 | Quantum teleportation between the Canary Islands La Palma and Tenerife over both quantum and classical 143-km free-space channels. **a**, Experimental scheme. Alice and Charlie are situated in La Palma, and Bob in Tenerife. Charlie prepares the teleportation input photon 1 in $|\phi\rangle_1$, using a heralded single-photon (HSP) source with a trigger photon 0 (photons are indicated by black numerals on red circles). An Einstein–Podolsky–Rosen (EPR)[23] source generates an entangled pair of photons 2 and 3 in the state $|\Psi^-\rangle_{23}$. Alice then performs a Bell-state measurement (BSM) on photons 1 and 2, and projects them onto two of the four Bell states ($|\Psi^-\rangle_{12}$/$|\Psi^+\rangle_{12}$), and sends the result via the classical feed-forward channel to Bob. Photon 3 is sent via the free-space quantum channel to Bob, who applies a unitary transformation (identity operation or π phase shift) on photon 3 depending on the BSM result and thus turns its state $|\phi\rangle_3$ into a replica of the initial quantum state $|\phi\rangle_1$. **b**, Set-up. In La Palma, a frequency-uncorrelated polarization-entangled photon pair source generated photons 2 and 3 in BBO_1 (EPR/Alice) and a collinear photon pair source generated photons 0 and 1 in BBO_2 (HSP/Charlie). All single photons were coupled into single-mode fibres. For implementing the BSM, photons 1 and 2 interfered in a fibre beam splitter (FBS) followed by polarization-resolving single-photon detection (BSM/Alice). Photon 3 was guided to the transmitter telescope via a 100-m single-mode fibre and sent to Bob in Tenerife, where the unitary transformation was implemented using an electro-optical modulator (EOM) and photon 3's polarization was measured. A real-time feed-forward operation was implemented by encoding the $|\Psi^+\rangle_{12}$ BSM result in 1,064-nm laser pulses, which were then sent to Bob via the feed-forward channel. On Bob's side, they were separated by a dichroic mirror (DM), detected with a photodetector (PD) and used to trigger the EOM to perform the required π phase shift operation. See main text for details.

Our experiment was conducted between Alice's transmitter station (at the Jacobus Kapteyn Telescope (JKT) of the Isaac Newton Group on La Palma) and Bob's receiver station (at the Optical Ground Station (OGS) of the European Space Agency on Tenerife), separated by 143 km, both at altitudes of about 2,400 m. Our experimental set-up is shown in Fig. 1b. At La Palma, near-infrared femtosecond pulses (with a central wavelength of 808 nm) emitted from a mode-locked Ti:sapphire laser, with a repetition rate of 80 MHz, were up-converted to blue pulses (with a central wavelength of 404 nm). They were used to generate two photon pairs via type-II spontaneous parametric down conversion (SPDC) in two nonlinear β-barium borate (BBO) crystals placed in sequence. The first SPDC source was aligned to emit the entangled auxiliary photon pairs (photons 2 and 3) in the $|\Psi^-\rangle_{23}$ state[24], equation (1), while the second crystal was a heralded single-photon (HSP) source providing Charlie's photon 1 to be teleported. That source delivered pairs of horizontally (photon 0) and vertically (photon 1) polarized photons in a product state. The detection of photon 0 by the avalanche photodiode (APD) t served as a trigger to herald the presence of photon 1. All photons were spectrally filtered using interference filters (IF) and coupled into single-mode fibres for spectral and spatial mode selection.

To realize the BSM, Alice's photon 2 was overlapped on a fibre beam splitter (FBS) with the teleportation input photon 1, whose polarization was arbitrarily prepared by Charlie using half- and quarter-wave plates (HWP and QWP). In each output port of the FBS, a polarizing beam splitter (PBS) was used to project these photons on either horizontal or vertical polarization. Fibre polarization controllers (FPCs) were used to compensate for unwanted polarization rotation induced

by the fibres. Our BSM can identify two out of the four Bell states, which is the optimum achievable with linear optics only[25]. For more details on our BSM, see Supplementary Information. While the BSM was being performed at Alice, photon 3 was guided to a 7-cm-aperture transmitter telescope through a 100-m-long single-mode fibre and then sent via a 143-km free-space quantum channel over to Bob in Tenerife. There, it was collected by the 1-m-aperture OGS telescope, and guided through its Coudé path to Bob.

In the first stage of our experiment, we only considered the cases where Alice detected $|\Psi^-\rangle_{12}$ in the BSM, which results in photon 3 being already in the state of the input photon, $|\phi\rangle_1$, and hence Bob was required to perform an identity operation, that is, to do nothing at all. We verified the success of the teleportation process by analysing the polarization state of photon 3, which was accomplished by a polarization analyser, consisting of a quarter- and a half-wave plate and two free-space coupled Si-APDs (silicon avalanche photodiodes) placed in each output mode of a polarizing beam splitter.

In the second stage of our experiment, we implemented a real-time feed-forward operation. When Alice obtained $|\Psi^+\rangle_{12}$, she sent this classical information to Bob. On receiving this information, Bob had to apply a π phase shift between the $|H\rangle$ and $|V\rangle$ components of photon 3 to obtain the replica of the input state $|\phi\rangle_1$. For further details on the feed-forward implementation, see Supplementary Information.

The relevant events on Alice's and Bob's sides were recorded with separate time-tagging units each disciplined to the global positioning system (GPS)[14]. First, Alice in La Palma identified the threefold coincidence events corresponding to the $|\Psi^{\pm}\rangle_{12}$ outcomes of the BSM. This was done using a coincidence logic circuit featuring two separate output signals realized with transistor-transistor logic (TTL) pulses. These TTL pulses were fed into a time-tagging unit which recorded the exact time and the BSM result into a binary file. Similarly, Bob fed either the signals of both detectors (stage 1, without feed-forward) or the coincidence between these signals and the BSM results sent via 1,064-nm laser pulses (stage 2, with feed-forward) into his time-tagging unit. After a measurement run was completed, both time-tagged data files were compared by cross-correlation, and the detection events associated with simultaneous detection of four photons originating from the same pump pulse were identified.

The real-life long-distance environment provided a number of challenges for the present teleportation experiment. These challenges resulted most significantly in the need to cope with an extremely low signal-to-noise ratio when using standard techniques—indeed, too low to perform a successful experiment. To enhance the signal-to-noise ratio to a level that made the experiment possible, we used the following advanced techniques: a frequency-uncorrelated polarization-entangled photon pair source[26–28], ultra-low-noise large-active-area single-photon detectors at Bob[29], and entanglement-assisted clock synchronization[13,14,17]. Whereas all these techniques have been implemented individually, our work is (to our knowledge) the first that combines all of them simultaneously and moreover in an outdoor environment. See Supplementary Information for details.

First we present our results without feed-forward, where we only considered the BSM outcome $|\Psi^-\rangle_{12}$. The input state $|\phi\rangle_1$ was always approximately one of the four ideal input states $|\phi_{\text{ideal}}\rangle \in \{|H\rangle, |V\rangle, |P\rangle = (|H\rangle + |V\rangle)/\sqrt{2}, |L\rangle = (|H\rangle - i|V\rangle)/\sqrt{2}\}$. We performed tomographic measurements on three consecutive nights, thereby accumulating data over 6.5 h. Figure 2 shows the state tomography results of quantum teleportation. The measured density matrix ρ for each of these teleported states was reconstructed from the experimentally obtained data using the maximum-likelihood technique[30]. The fidelity of the teleported state is defined as the overlap of the ideal teleported state $|\phi_{\text{ideal}}\rangle$ with the measured density matrix: $f = \langle\phi_{\text{ideal}}|\rho|\phi_{\text{ideal}}\rangle$. For this set of states, the teleported state fidelities are measured to be $f = 0.890(42)$, $0.865(46)$, $0.845(27)$ and $0.852(37)$, yielding an average $\bar{f} = 0.863(38)$, where digits in parentheses represent 1σ uncertainties, for example, $\bar{f} = 0.863 \pm 0.038$. During these measurements the link attenuation varied from 28.1 dB to 39.0 dB, which was mainly caused by rapid temperature change and strong wind. Despite such high loss in the quantum free-space channel, the classical average fidelity limit[9] of 2/3 was clearly surpassed by our observed fidelities, as shown in Fig. 3. (Note that our random sampling of the input states over the mutually unbiased bases states leads to the same classical limit as sampling over the whole Bloch sphere. Also, it does not matter whether the sampling is done over all six mutually unbiased basis states or over three states with one state per basis.) Therefore, we have explicitly demonstrated quantum teleportation over the 143-km free-space channel.

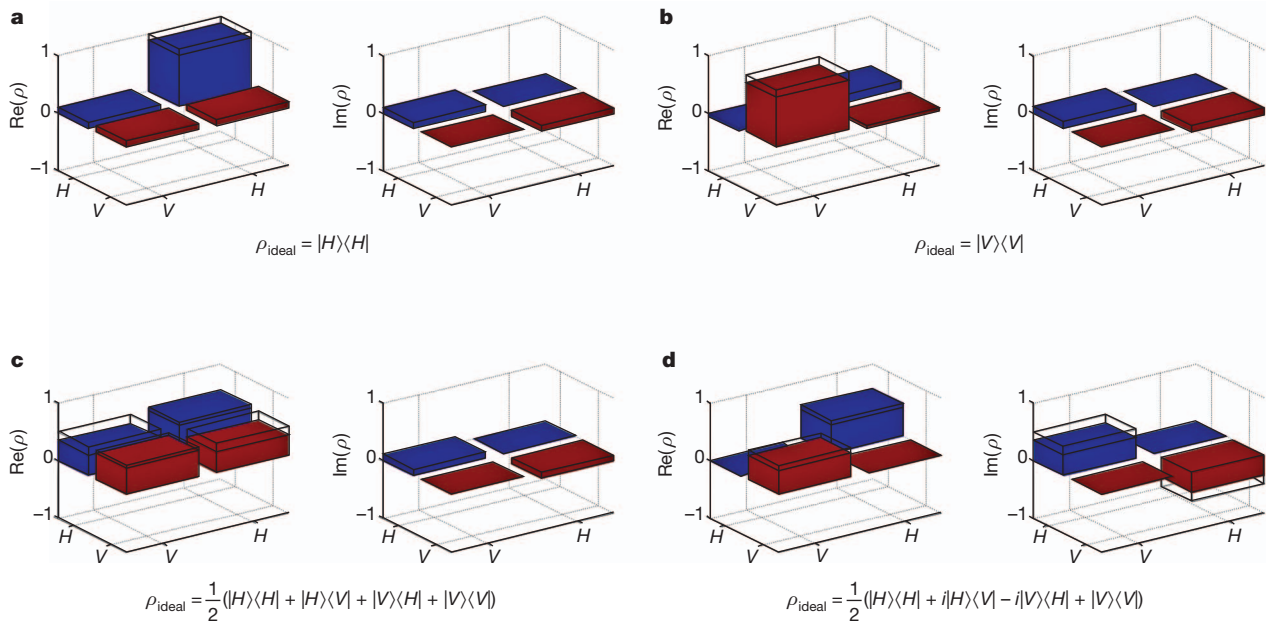

Figure 2 | State tomography results of the four quantum states without feed-forward over the 143-km free-space channel with the BSM outcome of $|\Psi^-\rangle_{12}$. The bar graphs show the reconstructed density matrices ρ for the four states teleported from Alice (La Palma) to Bob (Tenerife) over the 143-km free-space channel. The wire grid indicates the expected values for the ideal cases. The data shown comprise a total of 605 fourfold coincidence counts in about 6.5 h. The uncertainties in state fidelities extracted from these density matrices are calculated using a Monte Carlo routine assuming Poissonian errors.

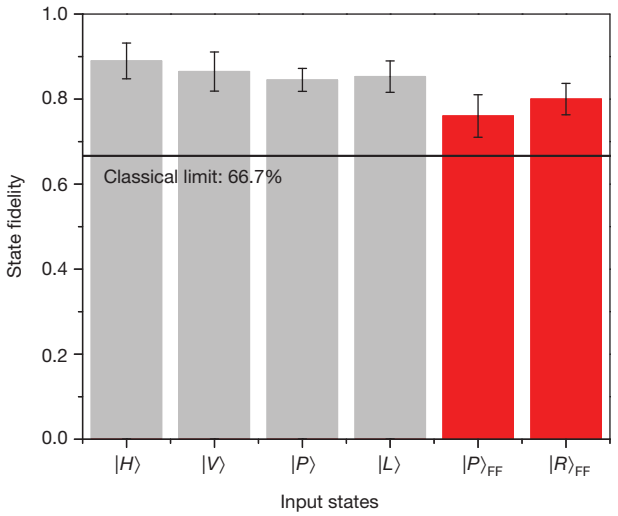

Figure 3 | Summary of the state fidelity results for the teleported quantum states with and without feed-forward. Grey bars show the results obtained in quantum teleportation without feed-forward. Bob was informed via an internet connection when Alice's BSM outcome was $|\Psi^-\rangle_{12}$, that is, those cases where he is not required to apply any operation to his photon. The uncertainties of these state fidelities are the same as presented in the main text. Red bars stand for the results obtained in quantum teleportation with feed-forward (FF). Bob was informed via the classical free-space link of Alice's BSM outcomes of $|\Psi^+\rangle_{12}$. The uncertainties of these state fidelities are derived from Poissonian statistics. All observed fidelities significantly exceed the classical average fidelity limit of 2/3 (66.7%). Error bars, $\pm 1\sigma$.

The reconstructed density matrices of the teleported quantum states allow us to fully characterize the teleportation procedure by quantum process tomography. The four input states ($\rho_{\mathrm{ideal}} = |\phi_{\mathrm{ideal}}\rangle\langle\phi_{\mathrm{ideal}}| = |H\rangle\langle H|, |V\rangle\langle V|, |P\rangle\langle P|, |L\rangle\langle L|$) are transferred to the corresponding (reconstructed) output states ρ. We can completely describe the effect of teleportation on the input states ρ_{ideal} by determining the process matrix χ, defined by $\rho = \sum_{l,k=0}^{3} \chi_{lk}\sigma_l\rho_{\mathrm{ideal}}\sigma_k$, where the σ_i are the Pauli matrices with σ_0 the identity operator. The process matrix χ can be computed analytically from these four equations for the four different input and output states[2]. The ideal process matrix of quantum teleportation χ_{ideal} has only one non-zero component, $(\chi_{\mathrm{ideal}})_{00} = 1$, meaning the input state is teleported without any reduction in quality. Figure 4a and b show respectively the real and imaginary components of χ for quantum teleportation based on our experimental results. The process fidelity of our experiment was $f_{\mathrm{process}} = \mathrm{Tr}(\chi_{\mathrm{ideal}}\chi) = 0.710(42)$. This clearly confirmed the quantum nature of our teleportation experiment as it is five standard deviations above the maximum process fidelity of 0.5, which is the limit one can reach with a classical strategy where Alice and Bob do not share any entanglement as a resource.

In the second stage of the experiment, we realized quantum teleportation including real-time feed-forward of the BSM result over the 143-km classical channel. We set $|P\rangle$ and $|R\rangle$ states ($|R\rangle = (|H\rangle + i|V\rangle)/\sqrt{2}$) as input states for which the required π phase shift between the $|H\rangle$ and the $|V\rangle$ components of photon 3 resulted in a 90° polarization rotation. However, for the $|H\rangle$ or $|V\rangle$ input state, feed-forward is irrelevant because a π phase shift would only result in a non-detectable global phase shift. Thus, the quality of teleportation of these states is already confirmed by our first-stage experiment. Realizing teleportation for the states $|P\rangle$ and $|R\rangle$ fully confirms the generality of the procedure, as these states belong to different mutually unbiased bases. In Tenerife, we analysed photon 3 in the eigenbasis of the input state, that is, the $|P\rangle/|M\rangle$ ($|R\rangle/|L\rangle$) basis when the input state was $|P\rangle$ ($|R\rangle$). Here $|M\rangle = (|H\rangle - |V\rangle)/\sqrt{2}$. The resultant fidelities of the teleported states are 0.760(50) and 0.800(37) for $|P\rangle$ and $|R\rangle$, respectively (red bars in Fig. 3). Both results are clearly above the classical fidelity bound. Note that in our experiment, the efficiency of the classical link was measured to be 21.3%, which was mainly due to amplitude fluctuations caused by atmospheric turbulence.

Using the real-time feed-forward operation, we unambiguously experimentally demonstrated quantum teleportation from La Palma to Tenerife over a 143-km free-space channel. We note that from a conceptual perspective, real-time feed-forward is part of the original teleportation proposal[5]. Ultimately, the advantage of long-distance teleportation compared to just sending the quantum state itself may lie in the following future applications: if Alice and Bob can stockpile their entangled states beforehand (with the help of quantum memories), teleportation is advantageous if the quantum channel is of low quality or if Bob's location is unknown to Alice. This is because Alice can broadcast the classical information with high quality and to arbitrary, or even unknown, locations[5]. (Also, the quantum repeater, which is of high importance for large-scale quantum networks, is based on teleportation in the form of entanglement swapping[31].) Specifically, this advantage also shows the usefulness of quantum teleportation even for quantum channels that allow only small transmission rates. We note that over the years teleportation sources have been markedly improved. We believe this development will continue and currently several new schemes are being pursued.

Our work proves the feasibility of both ground-based and satellite-based free-space quantum teleportation. Our quantum teleportation set-up was able to achieve coincidence production rates and fidelities sufficient to cope with the optical link attenuation resulting from various experimental and technical challenges; such challenges will arise in quantum transmission between a ground-based transmitter

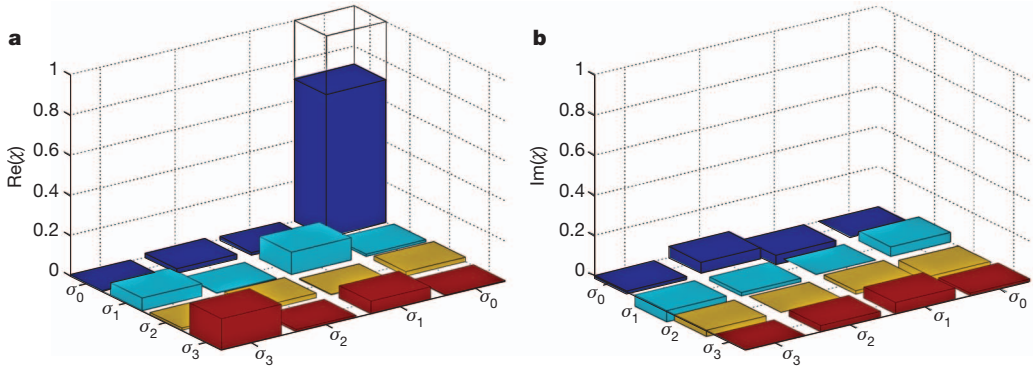

Figure 4 | Quantum process tomography of quantum teleportation without feed-forward. a, b, The real (Re(χ_{lk}); **a**) and imaginary (Im(χ_{lk}); **b**) values of the components of the reconstructed quantum process matrix, with $l, k = 0, 1, 2$, and 3. The results of the state tomography of the four teleported states, $|H\rangle$, $|V\rangle$, $|P\rangle$, $|L\rangle$, are employed to reconstruct the process matrix of quantum state teleportation. The operators σ_i are the identity ($i = 0$) and the x-, y-, and z-Pauli matrices ($i = 1, 2, 3$). For the ideal case, the only non-zero component of the process matrix of quantum teleportation, χ_{ideal}, is $(\chi_{\mathrm{ideal}})_{00} = 1$, which is indicated by the wire grid. Our experiment clearly confirmed that χ_{00} (identity operation) is indeed the dominant component and surpasses the classical limit.

and a low-Earth-orbiting satellite receiver[32]. In fact, some of the demands of our experiment were even more challenging than in satellite communication since there the atmospheric distances to be overcome are certainly shorter than the distance between Tenerife and La Palma. In addition, acquiring, pointing and tracking (APT) for diffraction-limited transmitter and receiver telescopes in space is a well-established technology. Therefore, our experiment represents a crucial step towards future quantum networks in space, which require space-to-ground quantum communication. During the finalization of our manuscript, a related work was reported[33] that used a 150-Hz APT system, while our APT system operated at a few hertz, yet fast enough to fulfil the specific requirements of our experiment. The most significant distinction between ref. 33 and the experiment presented in this Letter is our implementation of an active feed-forward technique. The technology implemented in both experiments has certainly reached the required maturity for both satellite and long-distance ground communication. We expect that many of the features implemented here will be important building blocks for a new area of experiments.

Received 21 May; accepted 14 August 2012.
Published online 5 September 2012.

1. Kimble, H. J. The quantum internet. *Nature* **453,** 1023–1030 (2008).
2. Nielsen, M. & Chuang, I. *Quantum Computation and Quantum Information* (Cambridge Univ. Press, 2000).
3. Gisin, N. & Thew, R. Quantum communication. *Nature Photon.* **1,** 165–171 (2007).
4. Ladd, T. D. *et al.* Quantum computers. *Nature* **464,** 45–53 (2010).
5. Bennett, C. H. *et al.* Teleporting an unknown quantum state via dual classical and Einstein-Podolsky-Rosen channels. *Phys. Rev. Lett.* **70,** 1895–1899 (1993).
6. Bouwmeester, D. *et al.* Experimental quantum teleportation. *Nature* **390,** 575–579 (1997).
7. Boschi, D., Branca, S., De Martini, F., Hardy, L. & Popescu, S. Experimental realization of teleporting an unknown pure quantum state via dual classical and Einstein-Podolsky-Rosen channels. *Phys. Rev. Lett.* **80,** 1121–1125 (1998).
8. Furusawa, A. *et al.* Unconditional quantum teleportation. *Science* **282,** 706–709 (1998).
9. Massar, S. & Popescu, S. Optimal extraction of information from finite quantum ensembles. *Phys. Rev. Lett.* **74,** 1259–1263 (1995).
10. Hughes, R. J. *et al.* Free-space quantum key distribution in daylight. *J. Mod. Opt.* **47,** 549–562 (2000).
11. Rarity, J. G., Tapster, P. R., Gorman P. M. & Knight, P. Ground to satellite secure key exchange using quantum cryptography. *N. J. Phys.* **4,** 82 (2002).
12. Aspelmeyer, M. *et al.* Long-distance free-space distribution of quantum entanglement. *Science* **301,** 621–623 (2003).
13. Marcikic, I., Lamas-Linares, A. & Kurtsiefer, C. Free-space quantum key distribution with entangled photons. *Appl. Phys. Lett.* **89,** 101122 (2006).
14. Ursin, R. *et al.* Entanglement-based quantum communication over 144 km. *Nature Phys.* **3,** 481–486 (2007).
15. Villoresi, P. *et al.* Experimental verification of the feasibility of a quantum channel between space and Earth. *N. J. Phys.* **10,** 033038 (2008).
16. Fedrizzi, A. *et al.* High-fidelity transmission of entanglement over a high-loss free-space channel. *Nature Phys.* **5,** 389–392 (2009).
17. Scheidl, T. *et al.* Feasibility of 300 km quantum key distribution with entangled states. *N. J. Phys.* **11,** 085002 (2009).
18. Jin, X.-M. *et al.* Experimental free-space quantum teleportation. *Nature Photon.* **4,** 376–381 (2010).
19. Scheidl, T. *et al.* Violation of local realism with freedom of choice. *Proc. Natl Acad. Sci. USA* **107,** 19708–19713 (2010).
20. Marcikic, I., de Riedmatten, H., Tittel, W., Zbinden, H. & Gisin, N. Long-distance teleportation of qubits at telecommunication wavelengths. *Nature* **421,** 509–513 (2003).
21. Ursin, R. *et al.* Quantum teleportation across the Danube. *Nature* **430,** 849 (2004).
22. Briegel, H.-J., Dür, W., Cirac, J. I. & Zoller, P. Quantum repeaters: the role of imperfect local operations in quantum communication. *Phys. Rev. Lett.* **81,** 5932–5935 (1998).
23. Einstein, A., Podolsky, B. & Rosen, N. Can quantum-mechanical description of physical reality be considered complete? *Phys. Rev.* **47,** 777–780 (1935).
24. Kwiat, P. G. *et al.* New high-intensity source of polarization-entangled photon pairs. *Phys. Rev. Lett.* **75,** 4337–4341 (1995).
25. Calsamiglia, J. & Lütkenhaus, N. Maximum efficiency of a linear-optical Bell-state analyzer. *Appl. Phys. B* **72,** 67–71 (2001).
26. Kim, Y.-H., Kulik, S. P., Chekhova, M. V., Grice, W. P. & Shih, Y. Experimental entanglement concentration and universal Bell-state synthesizer. *Phys. Rev. A* **67,** 010301(R) (2003).
27. Poh, H. S., Lim, J., Marcikic, I., Lamas-Linares, A. & Kurtsiefer, C. Eliminating spectral distinguishability in ultrafast spontaneous parametric down-conversion. *Phys. Rev. A* **80,** 043815 (2009).
28. Yao, X.-C. *et al.* Observation of eight-photon entanglement. *Nature Photon.* **6,** 225–228 (2012).
29. Kim, Y.-S., Jeong, Y.-C., Sauge, S., Makarov, V. & Kim, Y.-H. Ultra-low noise single-photon detector based on Si avalanche photodiode. *Rev. Sci. Instrum.* **82,** 093110 (2011).
30. White, A. G., James, D. F. V., Eberhard, P. H. & Kwiat, P. G. Nonmaximally entangled states: production, characterization, and utilization. *Phys. Rev. Lett.* **83,** 3103–3107 (1999).
31. Żukowski, M., Zeilinger, A., Horne, M. A. & Ekert, A. K. ''Event-ready-detectors'' Bell experiment via entanglement swapping. *Phys. Rev. Lett.* **71,** 4287–4290 (1993).
32. Aspelmeyer, M., Jennewein, T., Pfennigbauer, M., Leeb, W. R. & Zeilinger, A. Long-distance quantum communication with entangled photons using satellites. *IEEE J. Sel. Top. Quantum Electron.* **9,** 1541–1551 (2003).
33. Yin, J. *et al.* Quantum teleportation and entanglement distribution over 100-kilometre free-space channels. *Nature* **488,** 185–188 (2012).

Supplementary Information is available in the online version of the paper.

Acknowledgements We thank the staff of IAC: F. Sanchez-Martinez, A. Alonso, C. Warden, M. Serra and J. Carlos; and the staff of ING: M. Balcells, C. Benn, J. Rey, O. Vaduvescu, A. Chopping, D. González, S. Rodríguez, M. Abreu, L. González; J. Kuusela, E. Wille and Z. Sodnik; and J. Perdigues of the OGS and ESA. X.-S.M., T.J., R.U. and A.Z. thank S. Ramelow for discussions, P. Kolenderski for discussions on the SPDC source with the Bell-state synthesizer, S. Zotter for help during the early stages of the experiment, and R. Steinacker for meteorological advice. J.K. was supported by the EU project MALICIA. E.A. and V.M. thank C. Kurtsiefer and Y.-S. Kim for detector electronics design, J. Skaar for support, and the Research Council of Norway (grant No. 180439/V30) and Industry Canada for support. This work was made possible by grants from the European Space Agency (contract 4000104180/11/NL/AF), the Austrian Science Foundation (FWF) under projects SFB F4008 and CoQuS, and the FFG for the QTS project (no. 828316) within the ASAP 7 program. We also acknowledge support by the European Commission, grant Q-ESSENCE (no. 248095) and the John Templeton Foundation.

Author Contributions X.-S.M. conceived the research, designed and carried out the experiment, and analysed data. T.H., T.S. and D.W. carried out the experiment and analysed data. S.K., W.N., B.W. and A.M. provided experimental assistance during the early stage of the experiment. J.K. provided the theoretical analysis and analysed data. E.A. and V.M. developed the ultra-low-noise detectors. T.J. provided experimental and conceptual assistance, and conceived and developed the coincidence analysis code. R.U. conceived the research, planned and carried out the experiment and analysed data. A.Z. defined the scientific goals, conceived the research, designed the experiment and supervised the project. X.-S.M., T.H., T.S., J.K., R.U. and A.Z. wrote the manuscript with assistance from all other co-authors.

Author Information Reprints and permissions information is available at www.nature.com/reprints. The authors declare no competing financial interests. Readers are welcome to comment on the online version of the paper. Correspondence and requests for materials should be addressed to X.-S.M. (Xiaosong.Ma@Univie.ac.at) or A.Z. (Anton.Zeilinger@Univie.ac.at).